



Detection of high moisture content in multilayered timber elements by means of non-destructive imaging techniques

Federica Morandi¹, Andrea Gasparella¹, Massimo Garai², Nicolas Quaegebeur³, Patrice Masson³

¹ Faculty of Science and Technology, Free University of Bolzano-Bozen, Bolzano, Italy
federica.morandi@unibz.it, andrea.gasparella@unibz.it

² Department of Industrial Engineering, University of Bologna, Bologna, Italy
massimo.garai@unibo.it

³ GAUS, Department of Mechanical Engineering, Université de Sherbrooke, Sherbrooke, QC, Canada
nicolas.quaegebeur@usherbrooke.ca, patrice.masson@usherbrooke.ca

Abstract

This work aims at tuning a non-destructive inspection technique, based on vibroacoustic analysis, capable of detecting the presence of high moisture content in timber elements. Most of the inspection techniques currently used to identify the damage caused by water are based on local measurements; through a limited number of measurement positions, the method proposed here allows scanning a whole surface to detect the presence of water in localized regions. First, the direction-dependent dispersion relations characterizing the propagation media are estimated through experimental measurements. Then, a delay-and-sum imaging algorithm is implemented to estimate the shape of the waterfront related to wicking phenomena. The proof of concept is provided by testing a plywood panel that had been in contact with water and that displayed a clear sorption profile. The results show that the location of the waterfront can be accurately estimated and that, for the frequency range used for the evaluation, the simplifying assumption of a circular distribution of wavenumbers is valid.

Keywords: NDT, moisture content, timber construction, wavenumber characterization, imaging algorithm.

1 Introduction

One of the most relevant concerns regarding timber structures is durability. The presence of high levels of humidity in wood can be related to capillary uptake from the ground, condensation due to a wrong design of the envelope, or infiltration. Whatever the cause is, when wood is exposed to water or water vapor, its mechanical characteristics change. If wood has the possibility to drain and dry the excess of water, then the original characteristics of wood are easily restored. Conversely, when wood cannot dispose the excess water, it degrades quickly.

One of the most relevant concerns in timber structures, and especially in those made of Cross Laminated Timber (CLT), is the presence of humidity above a safety threshold. When the moisture content in timber is greater than 20 %, molds and fungi start to appear, compromising the structural performance of timber [3]. Since timber constructions have linings that cover both sides of the walls, too often when the damage is found it is too late for an intervention. Moreover, while for timber frame buildings the substitution of rotten elements is reasonably feasible, the substitution of CLT panels is an extremely invasive and expensive technique. Considering that CLT buildings are relatively new in the market, rehabilitation interventions on these structures is a quite new and challenging topic.

Most of the inspection techniques currently used to identify the damage caused by water are based on capacitance or resistance methods that allow to measure locally the moisture content of the inspected element [1].

This work aims at developing a Non-Destructive Testing (NDT) procedure, based on vibro-acoustic analysis, capable of detecting the presence of anomalous moisture content in timber elements. The basic concept is straightforward: when wood reaches a certain moisture content, its vibro-acoustic propagation characteristics changes. The interface determined by the change in impedance is in fact a new boundary that generates reflections. Therefore, through the quantification of these reflections, it is possible to determine if and where wood is dry or not.

This approach offers several advantages compared to the other available inspection techniques. Through the application of a permanent set of sensors on the element to be controlled, the monitoring can be continuous in time, the defect can be automatically localized, and finally the status of the structural element can be checked remotely. And most importantly, the defect can be spot even if the sensors are located away from the damage, with some limitations that are discussed in the following. These features are extremely relevant for the field of fault detection in smart buildings and in the field of management optimization.

This study is presented as a proof-of-concept, the main idea being focused on applying these testing methodologies to Cross-Laminated Timber elements.

2 Background

The characterization of wood at different moisture content has been the objective of extensive research in the forestry sector, for the classification of wood is based upon the measurement of the longitudinal wave velocity, which in turn depends on the moisture content of the wood. Hence, a proper estimate of correction factors to compensate for humidity is crucial for the forestry industry [2].

Guided waves-based techniques in NDT or Structural Health Monitoring (SHM) are widely used in ducts, seismic engineering, automotive and aerospace engineering. The use of arrays of sources and receivers allows detecting the presence of cracks, notches, and anomalous static behaviours.

The use of ultrasonic NDT techniques on timber requires attention for several reasons: (i) timber is per se an anisotropic material. Layered products can be assumed as orthotropic but the hypothesis of elliptical distribution of the wavenumber must be verified; (ii) timber is inhomogeneous, therefore one has to consider the dimension of the defects (knots, holes) acting as scatterers in relation to the inspection wavelength; (iii) the material is layered, therefore it must be verified that no propagation occurs in superficial layers; (iv) damping of timber limits long-distance wave propagation (v) fibre orientation, which might deviate from longitudinal, affects wave velocity.

The microstructure of wood must be carefully considered when analysing wave propagation for wavelength compared to the dimensions of the inhomogeneities. Luckily, the dimensions of cells, vessels, resin ducts and so on are extremely small compared to the wavelengths used for inspection in this work, and therefore can be neglected.

2.1 Water sorption in timber and influence on wave velocity

Generally, wood is characterized by the orientation of the cells and ducts along the grain, and by an axial distribution system. A cell that has reached a functional maturity is composed by the lumen, an empty space where all the living contents used to stay, and the cell walls.

Moisture Content (MC) is defined as:

$$MC = \frac{m_{water}}{m_{dry}} \cdot 100 (\%) \quad (1)$$

where m_{water} is the mass of water in wood and m_{wood} is the mass of the oven dry wood.

The MC of green wood can range from 30 % to 200 %, while dried planks used for the manufacturing of engineered wood products have a standard MC that ranges around 10-12 % [3].

Moisture in wood can exist as free water (liquid water or water vapor in cell lumina and cavities) or as bound water (within cell walls). The moisture content at which the cell walls are saturated, but no water exists in cell lumina is called the Fiber Saturation Point (FSP).

The rate of liquid water sorption depends on several factors. It is higher in the longitudinal direction, and it is strongly affected by the boundary conditions of the wood, as water displaces air in the lumina [4].

Unlike other classical construction materials, wood can shrink and swell depending on the moisture content, changing the amount of water that it can absorb; both mass and volume depend on the MC.

The FSP is considered as that moisture content above which the physical and mechanical properties of wood do not change anymore. The FSP of wood averages around 30 % MC for most commercial woods.

Several studies report empirical relations to compensate the velocity of longitudinal waves for the MC.

The velocity of stress waves propagating in solid wood drops as the MC increases, with a greater slope below FSP and with a less marked dependence above the FSP [5-7]. The Modulus of Elasticity (MOE), evaluated from the longitudinal wave velocity, remains almost constant above the FSP. Another interesting feature is that the ratio between the dynamic MOE and the static MOE is affected by the moisture content when MC is below FSP, while it assumes relatively constant values above FSP [5].

From these considerations, it is possible to infer that the detection capability of a vibro-acoustic measurement setup increases with increasing moisture content, and that when 30 % MC is reached, the apparatus would detect straightforwardly any further variation in mechanical properties.

3 Method

The objective of the present work is to implement an imaging algorithm for the detection of high MC in building elements, and in particular in mass timber elements, the substitution of which in the lifespan of a building would represent a serious drawback in terms of serviceability. The proof of concept was provided studying, under controlled laboratory conditions, a scaled laminated wood panel: a cherry plywood panel.

Cherry is a hardwood characterized by a fairly uniform texture and a high dimensional stability after drying, which oriented the choice to this high-quality panel.

The mechanisms of water sorption may change when considering other species of wood, but since the implementation of the method is done on a macroscopic scale, this choice is not expected to influence the results.

The cherry plywood panel is made of 10 layers of equal thickness, for a total thickness of 15.2 mm, and has density $\rho = 680 \text{ kg m}^{-3}$. From the master panel, smaller panels were cut in different sizes to perform the different measurements that are presented in this work. In particular, the results concerning wavenumber identification were obtained on a 1.22 x 1.22 m panel, while the setup for the imaging was installed on a smaller element (1.22 m by 0.61 m).

This high-quality plywood is characterized by a marked orthotropic behaviour and a high damping. In laminated wood panels, each layer has a different orientation. Capillary actions are stronger along the grain, but the reduced thickness of each layer together with the fact that cherry is a porous wood, helps make the water absorption homogeneous in the cross section.

To implement the imaging algorithm, several preliminary measurements were necessary. Some hypotheses concerning the orthotropic nature of the panel had to be verified. Furthermore, the imaging algorithm was implemented in the time domain, i.e., generating pulses centred at a specific frequency, and that calls for a deep insight regarding the choice of the frequency range to be investigated. The analysis was conducted following the steps listed below.

1. The complex velocity of different guided wave modes along several radial directions was detected to:
 - a. verify whether the orthotropic nature of the plate could be simplified as circular or elliptical.

- b. identify the cut-off frequency of the A1 mode, and therefore limiting from above the frequency range of interest.
 - c. evaluate damping (using plane wave excitation) to avoid making any assumption on the cylindrical propagation.
2. The frequency range of interest was narrowed by studying the intervals in which the complex reflection coefficients measured on the dry plate and the wet plate gave the highest difference.
 3. A Delay-and-Sum imaging algorithm was implemented, and the input parameters were tweaked until convergence.

4 Results

4.1 Wavenumber information

The extraction of wavenumber information was performed using Prony's analysis, a method that fits the signal acquired on a grid of equally spaced points to a sum of complex damped exponentials, allowing to determine at once wavenumber, amplitude, and damping information [8] under plane-wave assumption.

Measurements were conducted in the frequency domain along a linear array of 141 points with a spacing of 0.002 m, spanning a total length of 0.28 m. Measurements were repeated along 5 radial directions ranging from 0 (parallel to grain) to $\pi/2$ radians (perpendicular to grain). The source was a circular piezoelectric transducer with diameter 0.0145 m and the acquisition of the signals was performed using the 3D-Laser Doppler Vibrometer Polytec (3D LDV - Polytec PSV 500-3D). The panel had dimensions 1.22 m by 1.22 m.

The measurement setup is depicted in Figure 1. The bottom corners of the plate were simply supported while the upper corners were clamped. An aluminium support was assembled to guarantee a good contact between the piezo emitter and the plate, having no other contact point with the plate under test.



Figure 1 - Measurement setup for the determination of the dispersion relations in plywood. Panorama of the panel and the laser Doppler vibrometer, with detail of the clamping of the panel and detail of the fixing of the piezo.

In Prony analysis, the information on the propagating modes is stored in coefficients, whose number is suitably chosen in relation to the element under investigation. Therefore, the extraction of the information followed the process described below:

- The target propagating mode (the first anti-symmetric mode, A0) was identified and the relative dispersion curve was calculated theoretically, using Mindlin's theory for acoustically thick plates.
- A tolerance criterion was set to exclude outliers.
- The coefficients that describe the forward and the backward propagating waves are identified: for each point of the wavenumber vector k , the value that lies closer to the Mindlin's fit is taken and the associated coefficient is stored.
- The same coefficients are used to identify the respective amplitudes and the damping factors.

From Prony analysis, it was observed that the cut-off frequency of mode A1 lies at around 35 kHz. When implementing imaging algorithms, it is desirable to have a single-mode propagation to associate each frequency to only one group velocity. The analyzed frequency range was therefore limited to 35 kHz. The direction-dependent wavenumbers and damping coefficients are presented in Figure 2, for frequencies ranging from 9 to 30 kHz.

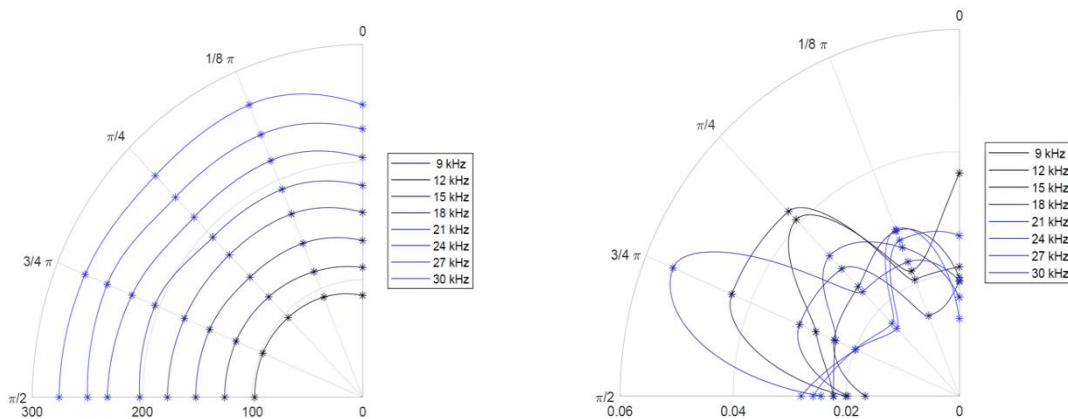


Figure 2 - Real (left) and imaginary (right) parts of the A_0 mode wavenumber measured along five radial direction in the cherry plywood plate. The direction labelled as “0” is parallel to the fibres of the face ply.

It is specified that, since measurements were performed using a circular piezo as source, damping information is affected by the geometrical spread of the wavefield. Measurements using a rectangular piezo bar were also performed along four directions (0 to $\frac{3}{4}\pi$ radians) to retrieve accurate estimates of damping.

4.2 Selection of the driving frequencies

Imaging algorithms are usually implemented in the time domain, generating bursts centered at specific frequencies.

The choice of a suitable frequency encapsulates several aspects. Imaging algorithms increase in precision when small wavelengths are used, but in plywood the cut-off frequencies of higher order Lamb waves modes are low.

A further refinement of the frequency range of investigation was performed through the analysis of the frequency region in which the mechanical characteristics of wet wood differ more from those of dry wood, through the analysis of the reflection coefficient, that was calculated according to Sherafat *et al.* [9].

The reflection coefficient is calculated, for each frequency, as the ratio of the amplitude of the reflected wave U_r to the amplitude of the incident wave U_i , corrected by a factor that compensates for the attenuation due to propagation:

$$R(\omega) = \frac{U_r(\theta_{inc}, \omega)}{U_i(\theta_{inc}, \omega)} e^{-k_I(\theta_{inc})d} \quad (2)$$

where θ is the angle of incidence, k_I is the imaginary part of the bending wavenumber of the propagating mode under analysis and d is the distance from the emitter to the center of the measurement array.

Amplitude and damping were estimated by measuring the spectral response of the plate to pseudo-random noise over a dense mesh of points (173 points spaced 0.0016 m apart) and using a rectangular piezo bar described above as source. The Prony analysis was used to evaluate the damping and the amplitude of the incident and scattered waves. Similarly, to what seen in the previous section, the data were extracted as follows:

- Identify the propagating wave.
- Fit the propagating wave using a theoretical model (Mindlin's plate).
- Set a tolerance criterion to exclude points that lie too far from the expected value.
- Identify of the coefficients that participate to the description of the forward propagating wave.
- Mirror the fitted curve to evaluate the backward propagating wave.
- Identify of the coefficients that participate to the description of the backward propagating wave.
- Use the same indices to evaluate the energy associated to the two waves.
- Estimate, with the same coefficients, of the damping (heavy smoothing required) and evaluation of the attenuation due to propagation.
- Calculate of the reflection coefficient according to Eq. 2.

Measurements were first performed on a dry board. Then, water was added in a basin that had been previously placed under the wood board, and the level of the water was raised until the lower edge of the panel was in contact with the water, adsorbing it by capillary action. It is worth noticing that this manipulation did not require the movement of any part of the equipment, and therefore did not require the calibration of the acquisition system. After five hours, the evaporation rate balanced the wicking and the water uptake profile remained constant. With this new modified boundary condition, the reflection coefficient was measured once again. The difference of the reflection coefficient calculated with and without water is shown in Figure 3. the regions in which the difference is maximum were selected as frequency ranges in which to generate pulses.

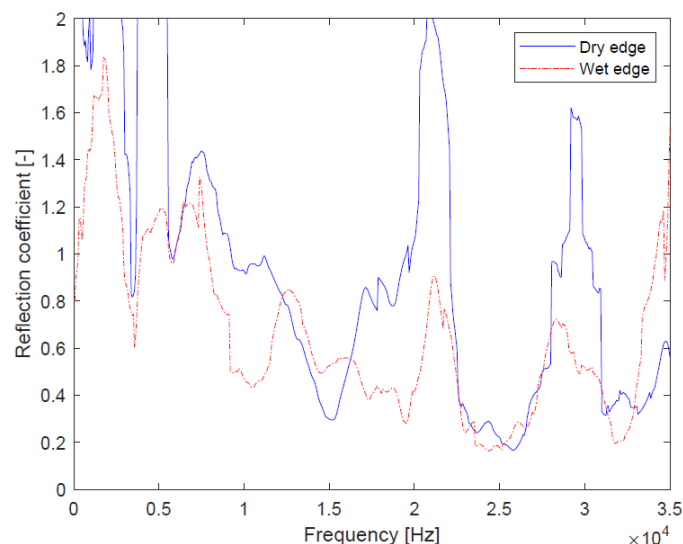


Figure 3 - Measured reflection coefficient in the $\theta_{inc} = 0^\circ$ direction on a cherry plywood panel having wet and dry edge.

From the analysis of the reflection coefficients, three optimal ranges of frequencies were identified, centered roughly around 10, 20 and 30 kHz, where the effect of water sorption marked the greatest influence on wave propagation.

A reasonable trade-off would be to choose the highest frequencies among these available, to increase the resolution of the method. Bursts were actually generated in all the identified frequency ranges, but results will be only shown at one frequency for the sake of brevity.

4.3 Implementation of a Delay-and-Sum imaging algorithm

A Delay-and-Sum (DAS) imaging algorithm was implemented following the formulation proposed by Michaels *et al.* [10] with some minor modifications.

The principle of this imaging technique is the calculation of the difference between two signals: one recorded on the healthy plate and one recorded, for the same set of transducers, on the damaged plate. The subtraction of the signals will generate a signal in which only the features that characterize the flaw are present: all direct components and the reflections from the boundaries are cancelled out. Therefore, the energy of the composite scattered field is calculated upon the so-called *differenced* signal in the following.

Consider a point source at position i and a receiver at position j on an isotropic plate. Under the hypothesis of a single mode propagation, the group velocity can be calculated as:

$$c_g = \frac{\sqrt{(x_i - x_j)^2 + (y_i - y_j)^2}}{t_{ij}} \quad (3)$$

where t_{ij} represents the time-of-flight from transducer i to transducer j , while x and y represent the spatial coordinates of the points.

If there is a flaw at position f , the signal recorded at position j will show a reflected component that will arrive at time t_{ij}^f :

$$t_{ij}^f = \frac{\sqrt{(x_i - x_f)^2 + (y_i - y_f)^2} + \sqrt{(x_j - x_f)^2 + (y_j - y_f)^2}}{c_g} \quad (4)$$

Given each pair of source-receiver transducers, for a defined group velocity, the distance that characterizes the flaw is identified by an ellipse that has the two points as foci.

The plate is then meshed into a set of points which are the coordinates of potential flaws: the scattered signal from all possible transducers' pairs is then summed up creating a matrix (s_{xy}) that represents the energy of the total scattered field:

$$s_{xy}(t) = \sum_{i=1}^{N-1} \sum_{j=i+1}^N d_{ij}(t - t_{ij}^f) w(t - t_{ij}^f) \quad (5)$$

where d_{ij} is the differenced signal and w is a windowing function.

Where more ellipses intersect, a flaw is localized, and the matrix will display a maximum.

Operationally, the impulse responses were acquired in the time domain. A cylindrical wave field was generated using a circular piezoelectric transducer (diameter 0.0145 m, thickness 0.003 m) and pseudo pulses (5-cycles Hanning-windowed sines) were generated at a central frequency of 20 kHz. Sixteen scanning points were randomly chosen on the panel and signals were acquired using again the 3D-Laser Doppler Vibrometer.

The signals were windowed to discard noisy tails and Time Gain Compensation (TGC) was applied to counteract for the attenuation due to propagation. Then, a matrix was built that, for each point of the mesh grid, estimated the time of arrival of a reflection from a potential flaw t_{ij}^f , with a spatial resolution of 0.2 cm.

For each of the measured signals, the envelope of the signal was calculated using the Hilbert transform and the value that it assumed at the specific time t_{ij}^f was calculated and summed up for all source-receiver combinations.

In this application, only one point source was considered and, instead of summing over a time window, the maxima of the envelopes are summed up. Eq. 5 is thus modified as:

$$s_{xy} = \sum_{i=1}^N d_{ij}(t_{ij}^f) \quad (6)$$

where N is the number of receivers.

The image is finally obtained by calculating, for each point of the matrix, the energy according to Eq. 5; where higher levels were found, a flaw was spot.

The water profile in the timber element and the preliminary results of the application of the imaging techniques are displayed in Figure 4. The algorithm clearly detected the presence of water in the lower region of the plate, where the energy of the total scattered field reaches a maximum. Figure 4a shows that, in the inner layers, the waterfront reached approximately 3 cm of height, with variations that depend on the orientation of the layers. The grid displayed on Figure 4b has a vertical resolution of 0.65 cm; the yellow-filled area covers 5 cells, indicating a total height of 3.25 cm. Future work will be devoted to improving the accuracy of the estimate of the waterfront. The low precision of the detection at the boundaries (i.e., the concave profile) is due to the construction of the ellipses: in particular, to the distribution of points, that were not generally picked close to the edges, and to the small dimensions of the plate. The orthotropic behavior of the plate has also been accounted for, but since the wavenumber variation is relatively small, the implementation of deformed ellipses did not improve the results relevantly.

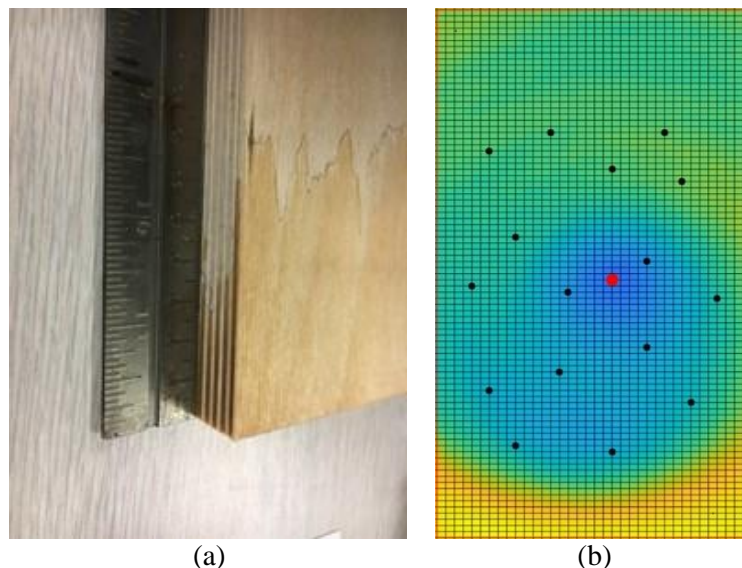


Figure 4 - Preliminary testing on a small plywood board. Water profile caused by wicking (a) and imaging results of the board (b), with the identification of the wet area in yellow. The red dot represents the position of the source piezo, while black dots represent the measurement points.

5 Conclusions

This work aimed at using a Non-Destructive Testing ultrasonic inspection technique to detect the presence of high moisture content in timber elements. To this aim, a multi-step procedure was followed comprising (i) the

characterization of wavenumber propagation on a timber plate, (ii) the determination of the optimal frequency range to inspect the plate, and (iii) the implementation of a delay-and-sum algorithm. The results of this preliminary testing show that the algorithm is able to detect the region characterized by a higher moisture content. The information related to the direction-dependent wavenumber did not improve the performance of the imaging algorithm. The analysis also showed that the identification of the frequency to use for inspection requires attention and should be tailored on the specific object tested. Future developments of the present work will regard the validation of the method by testing large scale Cross-Laminated Timber samples.

Acknowledgements

The authors wish to acknowledge the staff of the GAUS laboratories and Dr. Maxime Bilodeau for his precious support in the optimization of the measurement setup. This work was partially funded by the Interreg Italia-Austria Progetto V-A BIGWOOD ITAT1081.

References

- [1] Dietsch, P.; Franke, S.; Franke, B.; Gamper, A.; Winter, S. Methods to determine wood moisture content and their applicability in monitoring concepts. *Journal of Civil Structural Health Monitoring*, 5, 2015, 115-127.
- [2] Piazza, M.; Riggio, M. Visual strength-grading and NDT of timber in traditional structures. *Journal of Building Appraisal*, 3, 2008, 267-296.
- [3] Ross, R.J. (Ed.). *Wood Handbook - Wood as an Engineering Material*. General Technical Report FPL-GTR-190. United States Department of Agriculture, Forest Service, Forest Products Laboratory. Madison (WI), USA, 2010.
- [4] Zelinka, S.L.; Glass, S.V.; Boardman, C.R. Improvements to water vapor transmission and capillary absorption measurements in porous materials. *Journal of Testing and Evaluation*, 44, 2016, 2396-2402.
- [5] Wang X. Effects of size and moisture on stress wave E-rating of structural lumber. *Proceedings of the 10th World Conference on Timber Engineering*, Miyazaki, Japan, 2008.
- [6] Gonçalves R.; Mansini Lorensani, R.G.; Ottoboni Negreiros T.; Bertoldo C. Moisture-related adjustment factor to obtain a reference ultrasonic velocity in structural lumber of plantation hardwood. *Wood Material Science and Engineering*, 13(5), 2017, 254-261.
- [7] Llana D.F.; Íñiguez-González G.; Martínez R.D.; Arriaga F. Influence of timber moisture content on wave time-of-flight and longitudinal natural frequency in coniferous species for different instruments. *Holzforschung*, 72(5), 2017.
- [8] Parks, T.W. and Burrus, C.S. *Digital Filter Design*. Wiley, New York, USA, 1987.
- [9] Sherafat, M.H.; Quaegebeur, N.; Hubert, P.; Lessard, L.; Masson, P. Experimental model of impact damage for guided wave-based inspection of composites. *ASME J. Nondestructive Evaluation*, 1(4), 2018, 040801.
- [10] Michaels, J.E.; Michaels, T.E. Enhanced differential methods for guided wave phased array imaging using spatially distributed piezoelectric transducers. *Review of Quantitative Nondestructive Evaluation*, 25, 2006, 837-844.